International Journal of Control and Automation
Vol. 9, No. 9 (2016), pp.29-38
http//dx.doi.org/10.14257/ijca.2016.9.9.04

Brake Unit Driven by Magnetorheological Fluid Together with Shape Memory Alloy

Jianzuo Ma[1, 2, a,]*, Yunfei Liao[1, b] and Xiaofeng Cao[1, c]

[1] *College of Mechanical Engineering, Chongqing Industry Polytechnic College, Chongqing 401120, China*
[2] *School of Aeronautics and Astronautics, Chongqing University, Chongqing 400044, China*
[a]*mjzcqu@163.com*, [b]*14455325@qq.com*, [c]*602015822@qq.com*
** Corresponding Author: Jianzuo Ma*

Abstract

This paper aims to propose a brake unit driven by magnetorheological fluid together with shape memory alloy, based on the shape memory effect of shape memory alloy under thermal effect and the rheological behavior of magnetorheological fluid. The Bingham model is used to describe the constitutive characteristics of magnetorheological fluid subject to an applied magnetic field to derive the braking torque equation of brake induced by magnetorheological fluid. Based on the shape memory effect, the relationships of the shape memory alloy spring's output force with the temperature, the geometric parameters, the material parameters and the operating load is established to derive the braking torque equation of brake induced by shape memory alloy. The expression of the braking time is obtained from the torque-equilibrium equation of the braked shaft. The results indicate that the output force of the shape memory alloy spring can change rapidly with the temperature. The braking torque developed by shape memory alloy is increased with the increase of temperature. With the increase of the applied magnetic field strength, the braking torque developed by magnetorheological fluids goes up rapidly, and the braking time is shortened.

Keywords*: Shape memory alloy, Magnetorheological fluid, Brake unit, Braking torque, Braking time*

1. Introduction

Magnetorheological (MR) fluids and shape memory alloys (SMAs) are known as kinds of new intelligent materials because their properties can change rapidly with different external conditions [1, 2]. MR fluids are the suspension of micron-sized, magnetizable particles in a carrier fluid such as synthetic oil and silicone oil [3, 4]. In the absence of an applied magnetic field, MR fluids flow freely. When exposed to a magnetic field, the rheological characteristics of MR fluids reversibly and instantaneously change from a free-flowing liquid to a semi-solid with controllable yield strength. These fluids exhibit a viscoplastic behavior with the yield stress dependent upon strength of applied magnetic field. Altering the strength of the applied magnetic field precisely and proportionally controls the consistency or yield strength of the fluids [5, 6]. Based on the mechanical characteristics, the fluids can be used in the controllable, energy-dissipating applications such as brakes [7-9], valves [10], dampers [11] and clutches [12]. SMAs may undergo mechanical shape changes at relatively low temperatures and retain them until heated, then coming back to the initial shape [13]. This makes SMAs unique compared to other smart materials that can be used for actuator applications [14, 15].

ISSN: 2005-4297 IJCA

MR transmission devices are transmits torque by the shear stress of the MR fluids [16]. They have the properties that transmitting torque changes quickly in response to an external magnetic field. However, the transmission properties of MR fluid are affected by temperature greatly. In the operation of breaking, the thermal will disperse so much that heating the MR fluid filled in MR brake. The transmission performance of MR brake degraded or even failure in applied of high temperature. In order to overcome this shortcoming of MR brake, a brake unit driven by MR fluid together with SMA was present in this paper. The amount of the braking torque is provided by the MR fluid and SMA. The braking torque is mainly produced by MR fluid at low temperature. The friction torque induced by SMA is applied to compensate the loss torque of MR fluid at high temperature.

2. Operating Principle

The schematic of the brake unit driven by MR fluid together with SMA is shown as Figure 1. The transmission shaft and rotor-cylinder are initiative members, the shell is fixed. The MR fluid is filled with the full gap between two cylinders in the brake. In the absence of an applied magnetic field, MR fluids exhibit Newtonian-like fluid behavior. The torque transmitted by the viscous stress of the MR fluid in the brake is so small that the suspended particles of the MR fluid cannot restrict the rotor-cylinder motion of the brake. However, in the course of operation, a magnetic flux path is formed when electric current is put through the coil-assembly. As a result, the MR particles are gathered to form chain-like structures, in the direction of the magnetic flux path. These chain-like structures increase the shear stress of the MR fluid. With the increase of the applied magnetic field, the shear stress and torque developed by the MR fluids go up rapidly. The SMA spring and conventional steel spring are assembled as a biasing actuator. At relative low temperature, the conventional steel spring can deflect the SMA helical spring to its compressed length completely. The resilience of SMA helical spring is generated when the SMA spring is heated. The SMA springs provide normal force between two friction discs. The normal force increases rapidly with the increasing of temperature.

The amount of the braking torque for the brake unit driven by MR fluid together with SMA is provided by the MR fluid and SMA. The braking torque of MR brake can be controlled by an external magnetic field, however, the temperature range is narrow for MR fluid application, MR fluid prone to failure at high temperatures. The friction torque induced by SMA is applied to compensate the loss torque of MR fluid at high temperature. When the temperature is lower than 70℃, the braking torque is mainly provided by the MR fluid in the working gap. The braking torque can be continuously controlled by the applied magnetic field strength. When the temperature is between 70℃ and 150℃, the friction disks are engaged under the action of SMA spring, the braking torque is provided by the MR fluid together with SMA. When the temperature is higher than 150 ℃, MR fluid is failure at high temperature, and the SMA spring is gradually extended under the thermal effect, the braking torque is mainly provided by the SMA, the braking torque increases as the temperature rises.

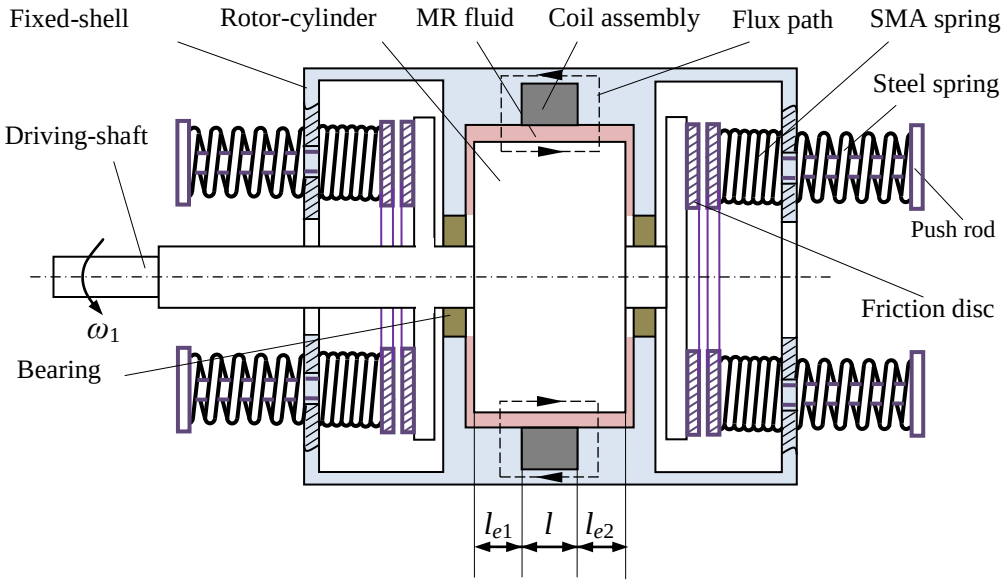

Figure 1. The Brake Unit Driven by MR Fluid Together with SMA

3. Braking Torque Induced by MR fluid

Figure 2 shows the circular flow of an MR fluid within the operational gap between two concentric cylinders. The inner cylinder radius is R_1, the outer cylinder radius is R_2, ((R_2-R_1) << R_1). When the inner cylinder is rotated at the velocity of ω_1, the MR fluid is sheared and flowed at the velocity of $\omega(r)$ in θ-direction. The braking torque is provided by the shear stress of the MR fluids.

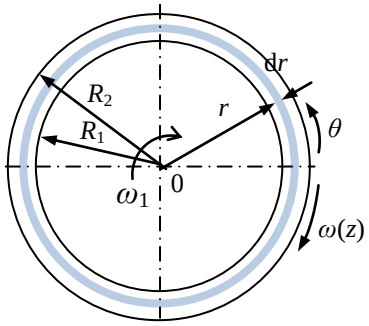

Figure 2. Flow Model of the MR fluid

In order to derive the equations of the fluid flow in the gaps between the rotor-cylinder and the fixed-cylinder in the brake, in cylindrical coordinates (r, θ, z), the following assumptions are given: the fluid is incompressible. There is no flow in r-direction and z-direction (v_r=0,v_z=0), but only tangential flow v_θ=$r\omega$ (r). The pressure of the MR fluid in the tangential direction is constant.

In radial the gap h, momentum equation can expressed approximately as

$$\frac{\mathrm{d}\tau_{r\theta}}{\mathrm{d}r}+\frac{2}{r}\tau_{r\theta}=0 \tag{1}$$

Where $\tau_{r\theta}$ is the shear stress of the MR fluid in the tangential direction.

MR fluid exhibits Newtonian behavior in the absence of an applied magnetic field. The shear stress of the MR fluid is governed by Newtonian's equation

$$\tau_{r\theta} = -\mu r \frac{\mathrm{d}\omega(r)}{\mathrm{d}r} \tag{2}$$

Where μ is the viscosity of MR fluid with no applied magnetic field.

Upon application of a magnetic flied, MR fluids exhibit a Bingham behavior. In this model, the flow of the MR fluid is governed by Bingham's equation

$$\tau_{r\theta} = \tau_y(H) - \mu r \frac{\mathrm{d}\omega(r)}{\mathrm{d}r} \tag{3}$$

Where $\tau_y(H)$ is the yield stress developed in response to an applied magnetic field.

Assume that the MR fluid exhibit yield shear flow in whole working gap between two cylinders. Submit Eq.(2) into Eq.(1), integrating Eq.(1) and applying the boundary conditions of $\omega(r)=\omega_1$ at $r=R_1$ and $\omega(r)=0$ at $r=R_2$, the flow velocity $\omega(r)$ can be mathematically manipulated to yield the flow as follow

$$\omega(r) = \frac{\omega_1 R_2^2 R_1^2}{R_2^2 - R_1^2}\frac{1}{r^2} - \frac{\omega_1 R_1^2}{R_2^2 - R_1^2} \tag{4}$$

For the shear flow of MR fluid in working gap between two cylinders, shown in Figure 2, the transmission torque of MR fluid at radius r can be expressed as

$$M = A\tau_{r\theta} r \tag{5}$$

Where A is the shear area.

MR transmission devices are usually designed such that the MR fluid can be magnetically saturated. The braking torque induced by MR fluid M can be divided into the yield stress component M_H developed by the applied magnetic field and the viscous component M_μ developed by the viscosity of MR fluids. When takes $r = \frac{R_2 + R_1}{2}$, the braking torque developed by the MR fluid can be obtain from Eq.s(3), (4) and (5) as follow

$$M = M_H + M_\mu = \frac{\pi L_e (R_2 + R_1)^2}{2}\tau_y(H) + \mu\frac{4\pi L \omega_1 R_1^2 R_2^2}{R_2^2 - R_1^2} \tag{6}$$

Where M is the braking torque, L_e is the effective length of the MR fluid exposed to the magnetic field, $L_e=l_{e1}+l_{e2}$. L is actual length of working gap in brake, $L=l_{e1}+l+l_{e2}$.

4. Braking Torque Induced by SMA

The most commonly used SMA elements for actuators are helical springs, for this form produces a large displacement. The shear strain γ for SMA spring can be expressed as:

$$\gamma = \frac{8\kappa F D}{\pi d^3 G(T)} \tag{7}$$

Here, the axial load is F, D is the average diameter of the spring, d represents the wire diameter, C is the spring index, $C=D/d$, κ is known as the Wahl correction factor applied, $\kappa = (4C\text{-}1)/(4C\text{-}4)+0.615/C$ and $G(T)$ is the shear modulus of SMA spring at temperature T.

The force that a spring of any material produces at a given deflection depends linearly on the shear modulus of the material. SMAs exhibit a large temperature

dependence on the material shear modulus. The relationship between shear modulus and temperature for SMAs is given by:

$$G(T)=\begin{cases} G_{\mathrm{M}} & \text{When } T<M_{\mathrm{f}} \text{ and } T<A_{\mathrm{s}} \\ G_{\mathrm{M}}+\dfrac{G_{\mathrm{A}}-G_{\mathrm{M}}}{2}[1+\sin\varphi(T-T_{\mathrm{m}})] & \text{When } M_{\mathrm{f}}\le T\le A_{\mathrm{f}} \\ G_{\mathrm{A}} & \text{When } T>A_{\mathrm{f}} \text{ and } T>M_{\mathrm{s}} \end{cases} \tag{8}$$

where, $G(T)$ is the shear modulus of SMA, T is temperature, M_{s}, M_{f}, A_{s} and A_{f} are the start and finish transformation temperatures of martensite and austenite respectively, G_{M} and G_{A} are the shear modulus of martensite and austenite respectively. In the process of heating, $T_{\mathrm{m}}=(A_{\mathrm{s}}+A_{\mathrm{f}})/2$, $\phi=\pi/(A_{\mathrm{f}}-A_{\mathrm{s}})$, In the process of cooling, $T_{\mathrm{m}}=(M_{\mathrm{s}}+M_{\mathrm{f}})/2$, $\phi=\pi/(M_{\mathrm{s}}-M_{\mathrm{f}})$.

The compressed length δ of SMA spring under the action of axial load F is given by:

$$\delta=\frac{8\kappa FD^3n}{d^4G(T)} \tag{9}$$

When $M_{\mathrm{f}}\le T\le A_{\mathrm{f}}$, the axial load of SMA spring at temperature can be obtained from Eq.(9) as

$$F(T)=\frac{\delta(T)G(T)}{\delta_{\mathrm{L}}G_{\mathrm{L}}}F_{\mathrm{L}} \tag{10}$$

Where, F_{L} is the axial load of SMA spring at low temperature.

$$F_{\mathrm{L}}=\frac{d^4G_{\mathrm{L}}}{8D^3n}\delta_{\mathrm{L}} \tag{11}$$

When the axial displacement of the SMA spring is limited, the amount of axial compressed length of spring is

$$\delta(T)=\delta_{\mathrm{L}} \tag{12}$$

When the displacement is restricted, the SMA spring output force can be obtained from Eqs.(10), (11) and (12) as

$$F(T)=\frac{G(T)d^4}{8D^3n}\delta_{\mathrm{L}} \tag{13}$$

For SMA spring actuator in Figure 1, the output displacement of SMA actuator is restricted. The SMA actuator export axial force when the SMA spring is heated. The normal pressure per unit area between driving and driven friction discs can be expressed as:

$$p=\frac{NG(T)d^4\left(\delta_{\mathrm{L}}-h\right)}{\pi\left(R_{f2}^2-R_{f1}^2\right)8D^3n} \tag{14}$$

Where, p is the normal pressure, N is the number of the SMA actuator, R_{f1} andR_{f2} are inner and outer radius of the friction disc, h is the initial gap between driving and driven friction discs.

The friction torque induced by SMA under the action of normal pressure p can be expressed as

$$M_f=\int_{R_{f1}}^{R_{f2}}2\pi fpr^2\mathrm{d}r=\frac{Nf\left(R_{f2}^3-R_{f1}^3\right)G(T)d^4\left(\delta_{\mathrm{L}}-h\right)}{12\left(R_{f2}^2-R_{f1}^2\right)D^3n} \tag{15}$$

Where f is the friction coefficient.

5. Results and Discussion

For the purpose of illustration, a typical MR fluid is used, its viscosity is μ=0.0925 Pa·s. The relationship between the yield stress and the applied magnetic field strength for typical MR fluid is shown in Figure 3. The yield stress of MR fluid is increased with the increase of applied magnetic field strength. The effect of temperature in output force of SMA spring is shown in Figure 4. In this study, the experimental system for testing the output force is shown in Figure 5. Ti-Ni SMA wire is used, its start and finish temperatures of the martensitic and austenitic phase transformation are M_s=120℃, M_f=70℃, A_s=85℃ and A_f=145℃, respectively. The shear modulus of martensite and austenite are G_M=7.5GPa and G_A=25GPa, respectively. The wire diameter of SMA spring is d=1.5mm, the average diameter of the spring is D=9mm, the number of turns is n=7. As show in Figure 4, the output force of SMA spring actuator increase with the increasing of temperature. The theoretical results are consistent with and experimental values, basically. The main errors are caused by: the manufacturing errors, the theoretical model error, and the measurement errors.

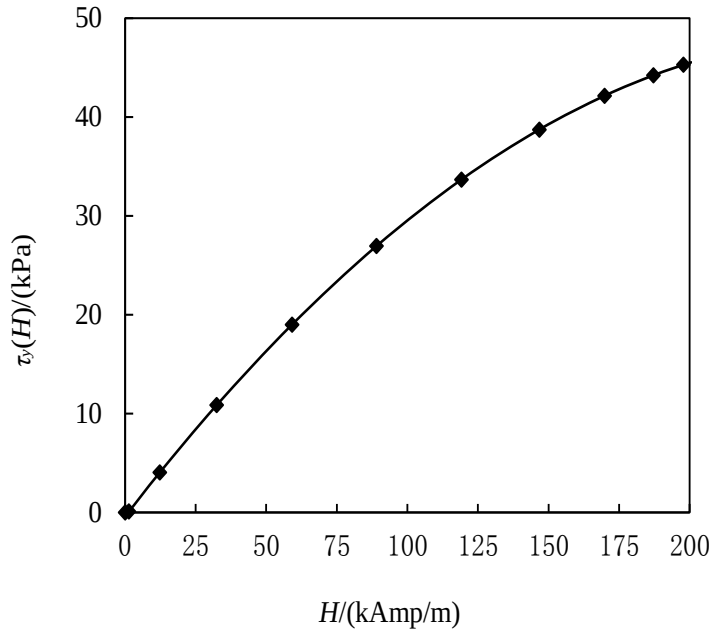

Figure 3. The Shear Stress versus Magnetic Field Strength

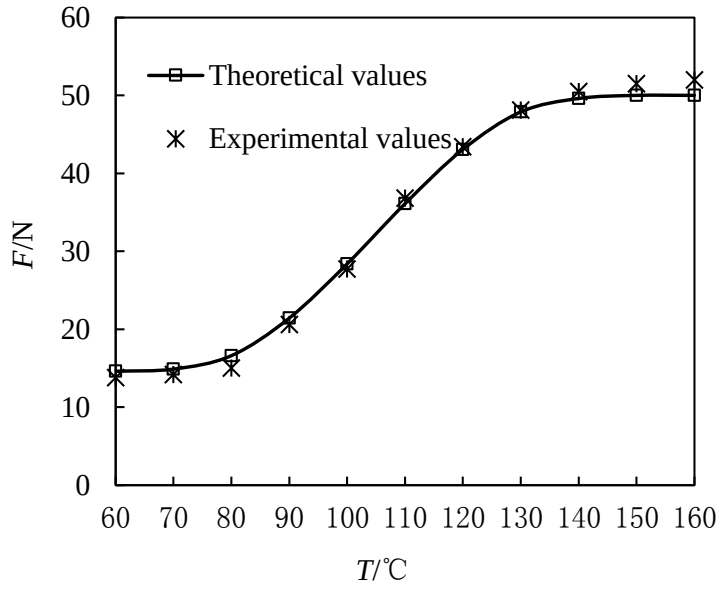

Figure 4. Output Force versus Temperature under the Constraint of Displacement

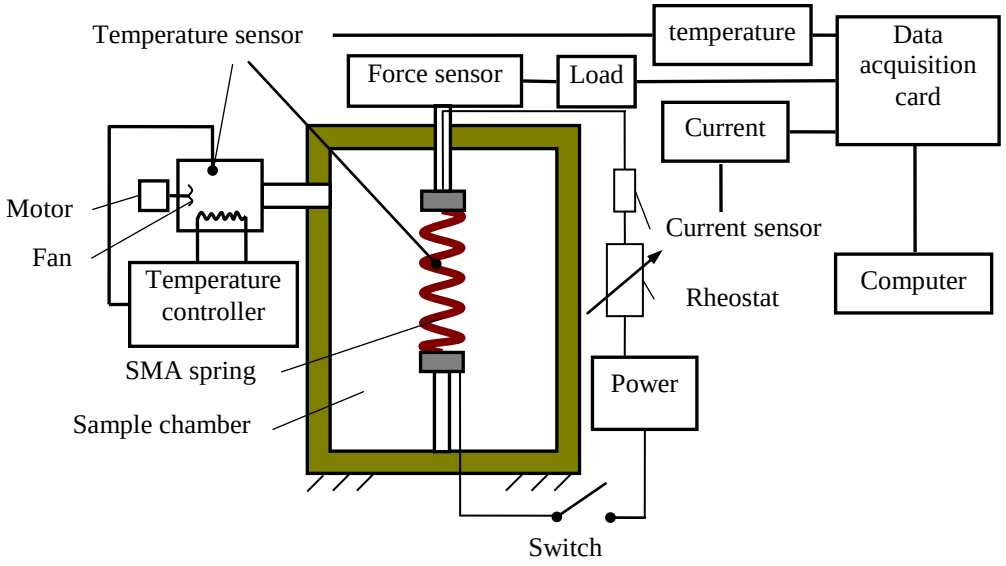

Figure 5. The Experimental System for Output Force of SMA Spring versus Temperature under the Constraint of Displacement

Figure 6 shows the relationship between the braking torque and the magnetic field strength for typical MR fluids. In this study, the following parameters are given: R_1=45mm, R_2=46mm, L=55mm, L_e=30mm. The rotational velocity ω_1=100rad/s. The braking torques developed by the typical MR fluid are 0.21N⊙m, 6.13N⊙m, 11.59N⊙m, 17.76 N⊙m, when the applied magnetic field strength are 0kAmp/m, 50 kAmp/m, 100 kAmp/m, 200 kAmp/m, respectively.

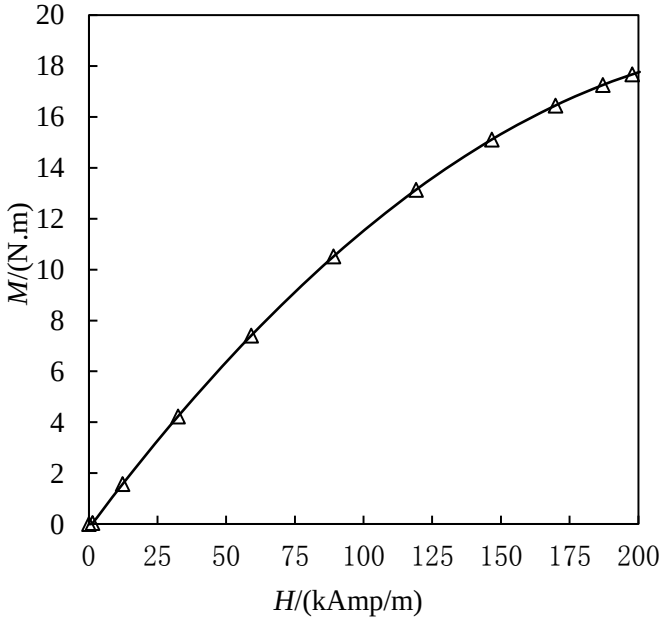

Figure 6. Braking Torque versus Magnetic Field Strength

The effect of temperature in friction torque of the brake is shown in Figure 7. Geometric parameters of the friction discs are: inner radius R_{f1}=35mm, outer radius R_{f2}=50mm, the initial gap h=1mm. the coefficient of friction between two discs is f=0.5. The initial force of bias steel spring is 15N. As shown in Figure 7, the friction torque of the brake is increased rapidly with the increase of temperature.

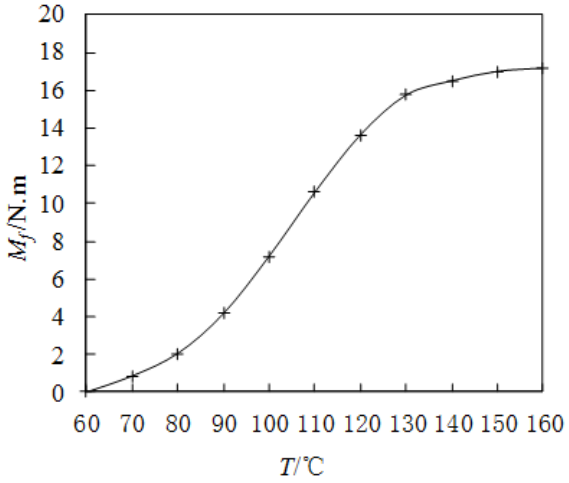

Figure 7. The Friction Torque versus Temperature

When the transmission torque of the braked shaft is M_b, the summation of transfer efficiency in transmission system is η_Σ, the braking time of the brake can be expressed as

$$t_b = \frac{J_{eq}\omega_1}{\psi\left(K_1\tau_y(H)+K_2\mu+M_f\right)+\left(\frac{1}{\eta_\Sigma}-1\right)M_b} \tag{16}$$

Where t_b is the braking time, ψ is the time coefficient of engagement, $0.5<\psi<1$, J_{eq} is the equivalent moment of inertia for the braked shaft. $K_1 = \frac{\pi L_e (R_2 + R_1)^2}{2}$, $K_2 = \frac{4\pi L \omega_1 R_1^2 R_2^2}{R_2^2 - R_1^2}$.

Figure 8 shows the effect of magnetic field strength on braking time at room temperature. In this study, ψ=0.9, η_Σ=0.97, M_b=15N·m, J_{eq}=0.3kg·m^2. The braking time are 65s, 4.7s, 2.5s and 1.8s, when the applied magnetic field strength are 0kAmp/m, 50 kAmp/m, 100 kAmp/m, 200 kAmp/m, respectively. The braking time is shortened with increase of an applied magnetic field.

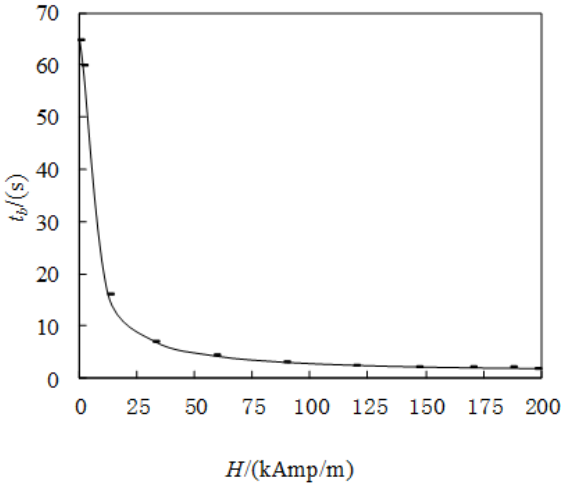

Figure 8. Braking Time versus Magnetic Field Strength

6. Summary

(1) A brake unit driven by MR fluid together with SMA is proposed full uses the properties of MR fluid and SMA to achieve a simple and reliable control of the braking torque and braking time.

(2) In the phase transition temperature range, the output force of the SMA spring is increased rapidly with the increase of temperature.

(3)The brake unit based on MR fluid and SMA can control the braking torque by applied magnetic field strength, meanwhile overcome the degradation of braking torque induced by MR fluid at high temperatures

Acknowledgments

This work was supported by the National Natural Science Foundation of China (51175532) and by Scientific and Technological Research Program of Chongqing Municipal Education Commission (Grant No. KJ1503104 and KJ1503109).

References

[1] S. Degeratu, P. Rotaru, Gh. Manolea, H. O. Manolea and A. Rotaru, "Thermal characteristics of Ni–Ti SMA (shape memory alloy) actuators", Journal of Thermal Analysis and Calorimetry, vol. 97, no. 2, **(2009)**, p. 695-700.
[2] W. Jiang, Y. Zhang and S. Xuan, "Dimorphic magnetorheological fluid with improved rheological properties", Journal of Magnetism and Magnetic Materials, vol. 323, no. 24, **(2011)**, pp. 3246-3250.
[3] A.G. Olabi and A. Grunwald, "Design and application of magneto-rheological fluid", Materials and Design, vol. 28, no. 10, **(2007)**, pp. 2658–2664.
[4] S. Chen, J. Huang, H. Shu, T. Sun and K. Jian, "Analysis and Testing of Chain Characteristics and Rheological Properties for Magnetorheological Fluid", Advances in Materials Science and Engineering, vol. 2013, **(2013)**, pp.1-6.
[5] J. Huang and Y. Yang, "Shear Transmission Properties of Magnetorheological Fluids between Two Parallel Disks", Disaster Advances, vol.6, no. 6, **(2013)**, pp. 284-291.
[6] J. Huang, P. Wang and G. Wang, "Squeezing Force of the Magnetorheological Fluid Isolating Damper for Centrifugal Fan in Nuclear Power Plant", Science and Technology of Nuclear Installations, vol.2012, **(2012)**, pp.1-6**.**
[7] J. Huang, J. Zhang, Y. Yang and Y. Wei, "Analysis and design of a cylindrical magneto-rheological fluid brake", Journal of Materials Processing Technology, vol.129, no.2, **(2002)**, pp. 559-562.
[8] K. Karakoc, E. J. Park and A. Suleman, "Design considerations for an automotive magnetorheological brake", Mechatronics, vol. 18, no. 8, **(2008)**, pp. 434–447
[9] J. Huang, J. He and G. Lu, "Analysis and Design of Magnetorheological Damper", Advanced Materials Research, vol. 148-149, no. 1, **(2011)**, pp. 882-886.
[10] D. Senkal and H. Gurocak, "Serpentine flux path for high torque MRF brakes in haptics applications", Mechatronics, vol. 20, no.3, **(2010)**, pp. 377-383**.**
[11] H. Hirani and C. S. Manjunatha, "Performance evaluation of a magnetorheological fluid variable valve", Proc. IMechE, vol. 221, no. 1, **(2007)**, pp. 83-93.
[12] J. Ma, G. Wang and D. Zuo, "Geometric Analysis in an MR Fan Clutch", Advanced Materials Research, vol. 239-242, no. 1, **(2011)**, pp. 1731-1734.
[13] G. Costanza, M.E. Tata and C. Calisti, "Nitinol one-way shape memory springs: Thermomechanical characterization and actuator design", Sensors and Actuators A, vol. 157, no. 1, **(2008)**, pp.113-117.
[14] D. Yu, B. Zhang, L. Jin, J. Liang and X. Wang, "Structural Design Method of Rotation Gear Actuated by Shape Memory Alloys", Journal of Mechanical Engineering, vol. 46, no. 14, **(2010)**, pp. 91-94.
[15] S. Dilthey and H. Meier, "Simulation-Based Design of a Rotatory SMA Drive", Journal of Materials Engineering and Performance, vol. 18, no.5, **(2009)**, pp. 686-690.
[16] J. Huang, X. Chen and L. Zhong, "Analysis and Testing of MR Shear Transmission Driven by SMA Spring", Advances in Materials Science and Engineering, vol. 2013, **(2013)**, pp. 1-6.

Authors

MA Jianzuo, he was born on January 7, 1983, in Zhejiang, China. Ph.D. of mechanical engineering. E-mail:mjzcqu@163.com

